Precise Predictions for Dijet Production at the LHC

J. Currie, A. Gehrmann-De Ridder, T. Gehrmann, E. W. N. Glover, A. Huss, and J. Pires

Precise predictions for dijet production at the LHC

J. Currie[a], A. Gehrmann-De Ridder[b,c], T. Gehrmann[c], E.W.N. Glover[a], A. Huss[b], J. Pires[d]

[a] *Institute for Particle Physics Phenomenology, University of Durham, Durham DH1 3LE, UK*
[b] *Institute for Theoretical Physics, ETH, CH-8093 Zürich, Switzerland*
[c] *Department of Physics, Universität Zürich, Winterthurerstrasse 190, CH-8057 Zürich, Switzerland*
[d] *Max-Planck-Institut für Physik, Föhringer Ring 6, D-80805 Munich, Germany*

We present the calculation of dijet production, doubly-differential in dijet mass, m_{jj} and rapidity difference, $|y^*|$, at leading colour in all partonic channels at next-to-next-to-leading order (NNLO) in perturbative QCD. We consider the long-standing problems associated with scale choice for dijet production at next-to-leading order (NLO) and investigate the impact of including the NNLO contribution. We find that the NNLO theory provides reliable predictions, even when using scale choices which display pathological behaviour at NLO. We choose the dijet invariant mass as the theoretical scale on the grounds of perturbative convergence and residual scale variation and compare the predictions to the ATLAS 7 TeV 4.5 fb^{-1} data.

The production of jets in the final-state is one of the most frequently occurring reactions at hadron colliders, such as the LHC. When at least two jets are produced, the two jets leading in transverse momentum, p_T, constitute a dijet system. Such systems are a powerful tool when searching for physics beyond the Standard Model by "bump hunting" in the dijet mass spectrum [1–4] or testing the QCD running coupling to very large momentum transfer [5, 6]. Even in the case of no new physics being found, dijet observables offer a win-win scenario as they can provide valuable information on important Standard Model parameters such as the strong coupling, α_s, and the Parton Distribution Functions (PDFs).

To fully exploit the wealth of available data it is important to have a reliable and accurate theoretical prediction. The dijet observables considered in this letter are currently known to NLO accuracy in perturbative QCD [7–11] and electroweak effects [12–14]. Although the NLO corrections give an improvement on the LO prediction, there remains significant theoretical uncertainty associated with the NLO calculation. It is well known that the parametric choice of scales for renormalization, μ_R, and factorization, μ_F, has a big impact on the predictions at NLO and, for this reason, the dijet data is regularly excluded from global PDF fits. To improve the theoretical description of dijet observables and make a meaningful comparison to data it is therefore necessary to calculate dijet production to NNLO accuracy. The NNLO correction to jet production was first discussed in the context of the single jet inclusive cross section [15, 16] and in this letter we report, for the first time, the NNLO corrections to dijet production.

At hadron colliders, jets are reconstructed by applying a jet algorithm [17] and ordered in transverse momentum. The LHC experiments have measured dijet events [18, 19] at 7 TeV as distributions in the dijet invariant mass, m_{jj},

$$m_{jj}^2 = (p_{j_1} + p_{j_2})^2, \tag{1}$$

where $p_{j_{1,2}}$ are the four-momenta of the two leading jets in an event satisfying the fiducial cuts, and the rapidity difference, $|y^*|$, where,

$$y^* = \frac{1}{2}(y_{j_1} - y_{j_2}), \tag{2}$$

and $y_{j_{1,2}}$ are the rapidities of the two leading jets. For two exactly balanced (back-to-back) jets, the invariant mass is related to the transverse momentum, p_T, and y^* variables by the simple relation,

$$m_{jj} = 2p_T \cosh(y^*). \tag{3}$$

This relation always holds at leading order (LO) but is modified at NLO and NNLO by the presence of additional real radiation contributions. It is evident from Eq. (3) that a minimum p_T cut translates to a minimum accessible value of m_{jj} which increases with $|y^*|$, such that in bins of large $|y^*|$ only large values of m_{jj} are experimentally accessible.

The longitudinal momentum fractions of the incoming partons can, for back-to-back jets, be written in terms of the final-state jet parameters using momentum conservation,

$$x_1 = \frac{1}{2}x_T \left(e^{+y_{j_1}} + e^{+y_{j_2}}\right) = x_T\, e^{+\bar{y}} \cosh(y^*),$$

$$x_2 = \frac{1}{2}x_T \left(e^{-y_{j_1}} + e^{-y_{j_2}}\right) = x_T\, e^{-\bar{y}} \cosh(y^*), \tag{4}$$

where $x_T = 2p_T/\sqrt{s}$ and $\bar{y} = \frac{1}{2}(y_1 + y_2)$ is the rapidity of the dijet system in the lab frame. From Eq. (4) it is clear that for small values of $\bar{y}$ the dijet data probe the configuration $x_1 \approx x_2$, with the x-values determined by the p_T of the jets. For large rapidities the data probes the scattering of a high-x parton off a low-x parton. By binning the data in $|y^*|$, these configurations are smeared out across the distribution and so a single bin in $|y^*|$ will contain a wide range of possible x-values. This is in contrast to binning in the maximum rapidity $y_{\max}$, as
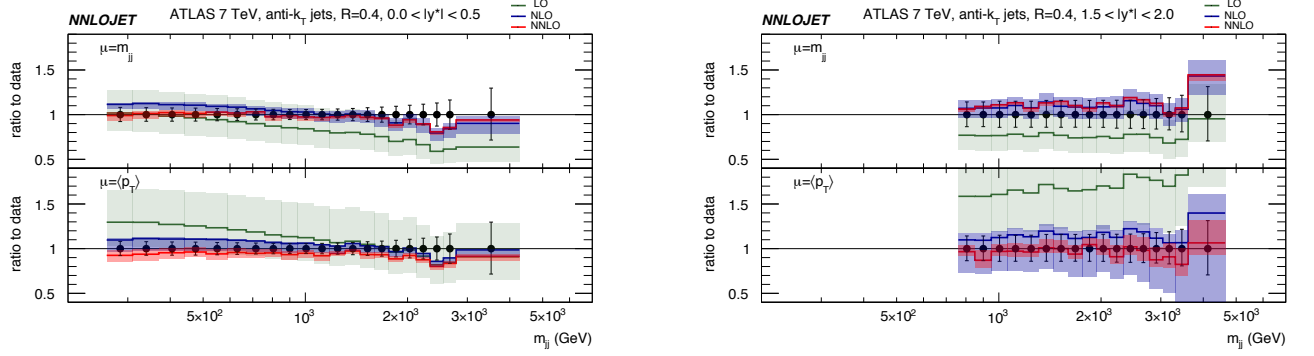
FIG. 1: Ratio of theory predictions to data for $0.0 < |y^*| < 0.5$ (left) and $1.5 < |y^*| < 2.0$ (right) for the scale choices $\mu = m_{jj}$ (top) and $\mu = \langle p_T \rangle$ (bottom) at LO (green), NLO (blue) and NNLO (red). Scale bands represent variation of the cross section by varying the scales independently by factors of 2 and 0.5.

was done for dijet studies at the DØ experiment [20], or the triply differential distribution in p_{T_1}, y_1 and y_2 (or alternatively, average jet p_T, $|y^*|$ and $|\bar{y}|$) [21, 22], which would provide more specific information on the x-values probed.

The data sample we compare to is the ATLAS 7 TeV 4.5 fb^{-1} 2011 data [19]. This constitutes the recording of all events with at least two jets reconstructed in the rapidity range $|y| < 3.0$ using the anti-k_t algorithm with R=0.4 such that the leading and subleading jets satisfy a minimum p_T cut of 100 GeV and 50 GeV respectively.

As detailed in [15], we include the leading colour NNLO corrections in all partonic sub-processes. The calculation is performed in the NNLOJET framework, which employs the antenna subtraction method [24, 25] to remove all unphysical infrared singularities from the matrix elements [26–28]. We use the MMHT2014 NNLO parton distribution functions [30] with $\alpha_s(M_Z) = 0.118$ for all predictions at LO, NLO and NNLO to emphasize the role of the perturbative corrections at each successive order.

At any given fixed order in perturbation theory, the predictions retain some dependence on the unphysical renormalization and factorization scales. The natural physical scale for dijet production is the dijet invariant mass, $\mu = m_{jj}$, which has not been widely used in dijet studies to date. Another scale, which was used at DØ [20] and is currently used by CMS [18] is the average p_T of the two leading jets, $\mu = \langle p_T \rangle = \frac{1}{2}(p_{T_1} + p_{T_2})$.

In Fig. 1 we show the predictions at LO, NLO and NNLO for these two scale choices at small and large $|y^*|$. For small $|y^*|$, both scale choices provide reasonable predictions with largely overlapping scale bands, reduced scale variation at each perturbative order, convergence of the perturbative series and good description of the data. For the larger $|y^*|$ bin we see significant differences in the behaviour of the predictions for the two scales. For the $\mu = m_{jj}$ scale choice, the behaviour is qualitatively similar to what is seen at small $|y^*|$; in contrast, the NLO prediction with $\mu = \langle p_T \rangle$ falls well away from the LO

prediction and is even outside the LO scale band. For this scale choice, the NLO contribution induces a large negative correction, which brings the central value in line with the data but with a residual scale uncertainty of up to 100%. Indeed for $|y^*| > 2.0$ the scale band for $\mu = \langle p_T \rangle$ widens further and even includes negative values of the cross section. These issues are resolved by the inclusion of the NNLO contribution such that the NNLO prediction is positive across the entire phase space and provides a good description of the data. With the issue of unphysical predictions resolved, we are free to make a scale choice based upon more refined qualities such as perturbative convergence and residual scale variation. On this basis we choose the theoretical scale $\mu = m_{jj}$ and present detailed results using this scale choice throughout the rest of this letter. It should be noted that these findings on the scale dependence can not be transferred to single-jet inclusive production [15], which is a completely different observable: each event contributes exactly once
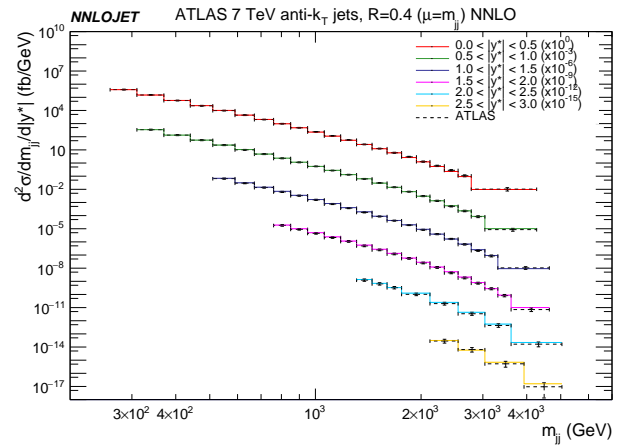

FIG. 2: The dijet cross section as a function of invariant mass, m_{jj}, for the six bins of $|y^*|$, compared to ATLAS 7 TeV 4.5 fb^{-1} data.
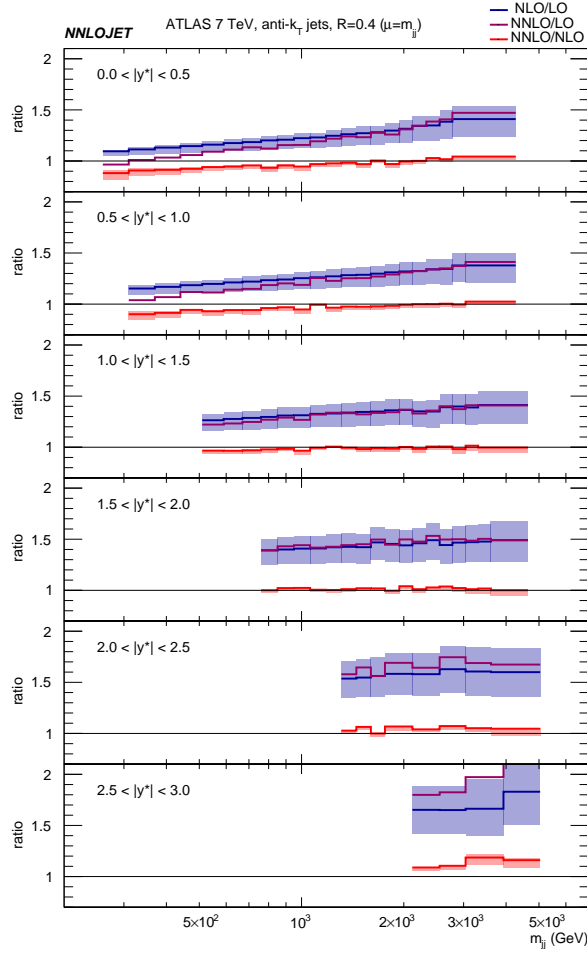
FIG. 3: NLO/LO (blue), NNLO/NLO (red) and NNLO/LO (purple) K-factors double differential in m_{jj} and $|y^*|$. Bands represent the scale variation of the numerator. NNLO PDFs are used for all predictions.
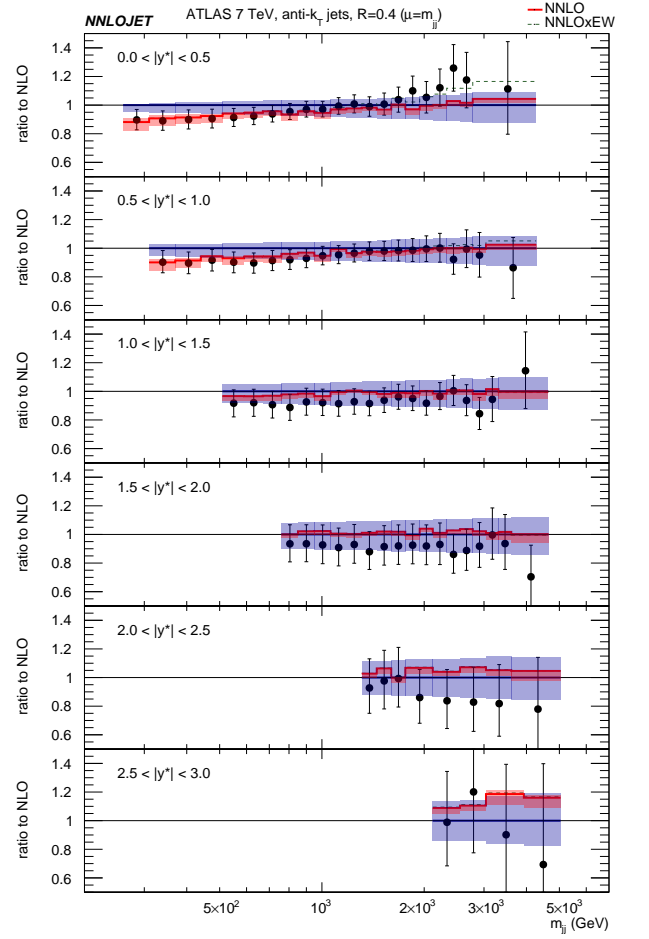
FIG. 4: The NLO (blue) and NNLO (red) theory predictions and ATLAS data normalized to the NLO central value. The bands represent the variation of the theoretical scales in the numerator by factors of 0.5 and 2. Electroweak effects are implemented as a multiplicative factor and shown separately as the green dashed line.

to the di-jet production, while yielding multiple entries with different kinematical variables (and consequently a much broader range of scale choice) in the single-jet inclusive cross section.

In Fig. 2 we present the absolute cross section as a function of m_{jj} for each $|y^*|$ bin, compared to NNLO-accurate theory. We observe excellent agreement with the data across the entire kinematic range in m_{jj} and $|y^*|$, with up to seven orders of magnitude variation in the cross section. The total NNLO prediction shown in Fig. 2 is the sum of LO, NLO and NNLO contributions. We can understand the relative shift in the theoretical prediction from each perturbative correction by examining the K-factors shown in Fig. 3. We observe moderate NLO/LO corrections from +10% at low m_{jj} and $|y^*|$ to +50-70% at high m_{jj} and high $|y^*|$. The NNLO/NLO K-factors are typically < 10% in magnitude and relatively flat, although they alter the shape of the prediction at low m_{jj} and low $|y^*|$.

To emphasize the size and shape of the NNLO correction, in Fig. 4 we show the distributions normalized to the NLO prediction. On the same plot we show the published ATLAS data, also normalized to the NLO theory prediction. We observe good agreement with the NNLO QCD prediction across the entire dynamical range in m_{jj} and $|y^*|$ and a significant improvement in the description of the data for low m_{jj} and $|y^*|$, where NLO does not adequately capture the shape nor the normalization. We include the electroweak effects as a multiplicative factor, as calculated in [12], and note that in the region where they are non-negligible ($|y^*| < 0.5$, $m_{jj} > 2$ TeV) they improve the description of the data.

We generally observe a large reduction in the scale variation and small NNLO corrections. An exception to this conclusion is found at low m_{jj} and $|y^*| < 1.0$; in this case we observe NNLO scale bands of similar size to the NLO bands, and a negative correction of approximately
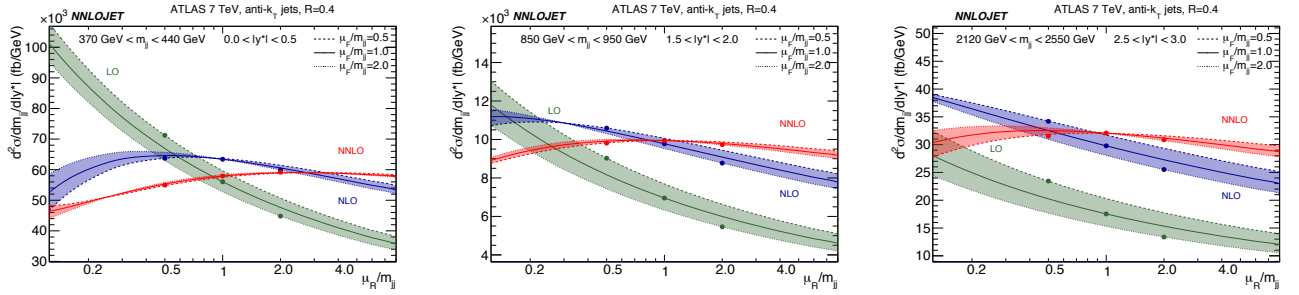
FIG. 5: The cross section evaluated in three bins as a function of μ_R/m_{jj}: 370 GeV $< m_{jj} <$ 440 GeV, $0.0 < |y^*| < 0.5$ (left); 850 GeV $< m_{jj} <$ 950 GeV, $1.5 < |y^*| < 2.0$ (centre); 2120 GeV $< m_{jj} <$ 2550 GeV, $2.5 < |y^*| < 3.0$ (right). The variation of the cross section, for fixed μ_F/m_{jj}, from the central value is shown as solid lines, computed from the renormalization group equation, for LO (green), NLO (blue) and NNLO (red). The thickness of the bands shows the variation due to factorization scale, with boundaries given by $\mu_F/m_{jj} = 0.5$ (dashed) and $\mu_F/m_{jj} = 2.0$ (dotted). The points show the NNLOJET result evaluated at $\mu_R/m_{jj} = \mu_F/m_{jj} = \{0.5, 1, 2\}$.

10% such that the NNLO and NLO scale bands do not overlap. To understand this behaviour in more detail we investigate specific bins of m_{jj} and $|y^*|$ and study the scale variation inside that bin, as shown in Fig. 5.

The left pane of Fig. 5 shows the scale variation in the bin 370 GeV $< m_{jj} <$ 440 GeV and $0.0 < |y^*| < 0.5$, which is the region where the NLO and NNLO scale bands do not overlap. For fixed μ_F it is clear that the central scale choice $\mu_R = m_{jj}$ lies close to the extremum of the NLO curve; and the predictions for upper and lower variations of μ_F cross each other in the vicinity of this central scale. As a consequence, the NLO scale variation both in μ_R and μ_F is accidentally minimized. The shape of the NLO curve also ensures that the scale variation is asymmetric, which can be seen in the corresponding bin in Fig. 4. Notwithstanding the variation in the range $0.5 < \mu_R/m_{jj} < 2$, the NNLO curve is clearly flatter and displays less variation than the NLO curve over the full range shown in the left pane of Fig. 5. This suggests that the non-overlapping NLO and NNLO scale bands in this bin is due to the NLO band underestimating the theoretical uncertainty whereas the NNLO band provides a more reliable estimate. The centre and right panes of Fig. 5 show the same quantities in bins of larger m_{jj} and $|y^*|$ and we see that in these bins the central scale choice $\mu_R = m_{jj}$ does not lie near the extremum of the NLO curve, and far away from a crossover point, so we obtain a more reliable NLO scale variation. We see that the NNLO curves are once again flatter and so we obtain a significant reduction in the scale variation with overlapping NLO and NNLO scale bands.

In summary, we have presented the first calculation of dijet production doubly differential in m_{jj} and $|y^*|$ at NNLO and compared to the available ATLAS data. We find that the ambiguities and pathologies of the theory prediction for certain scale choices at NLO, in particular the $\mu = \langle p_T \rangle$ scale choice, are removed by including the NNLO contribution. We find that the scale choice

$\mu = m_{jj}$ provides a nicely convergent perturbative series with significant reduction in scale variation at each order in perturbation theory. In particular, the NNLO scale uncertainty is smaller than the experimental uncertainty for this observable. Overall we observe small NNLO effects which are reasonably flat in m_{jj} and excellent agreement with the data, with the only exception being at low m_{jj} and low $|y^*|$ where the moderate NNLO correction improves the description of the data. In this region the NLO and NNLO scale bands do not overlap but this can be accounted for by the NLO scale band underestimating the perturbative theory uncertainty; whereas we expect the NNLO scale band does provide a reliable estimate.

It is clear from considering the theoretical uncertainty arising from the parameterization of the scale choice, and the scale variation about that central scale, that we obtain a reliable theoretical prediction for dijet production for the first time at NNLO. In doing so, the calculation reported here clears the way for previously unavailable phenomenological studies using dijet data.

[1] G. Aad *et al.* [ATLAS Collaboration], Phys. Rev. D **91**, 052007 (2015).

[2] V. Khachatryan *et al.* [CMS Collaboration], Phys. Rev. D **91**, 052009 (2015).

[3] G. Aad *et al.* [ATLAS Collaboration], Phys. Lett. B **754**, 302 (2016).

[4] A. M. Sirunyan *et al.* [CMS Collaboration], Phys. Lett. B **769**, 520 (2017).

[5] S. Chatrchyan *et al.* [CMS Collaboration], Eur. Phys. J. C **73**, 2604 (2013).

[6] [ATLAS Collaboration], ATLAS-CONF-2013-041.

[7] S. D. Ellis, Z. Kunszt and D. E. Soper, Phys. Rev. Lett. **69**, 1496 (1992).

[8] W. T. Giele, E. W. N. Glover and D. A. Kosower, Phys. Rev. Lett. **73**, 2019 (1994).

[9] Z. Nagy, Phys. Rev. Lett. **88**, 122003 (2002); Phys. Rev. **D68**, 094002 (2003).

[10] S. Alioli, K. Hamilton, P. Nason, C. Oleari and E. Re, JHEP **1104**, 081 (2011).

[11] J. Gao, Z. Liang, D. E. Soper, H. L. Lai, P. M. Nadolsky and C.-P. Yuan, Comput. Phys. Commun. **184**, 1626 (2013).

[12] S. Dittmaier, A. Huss and C. Speckner, JHEP **1211**, 095 (2012).

[13] J. M. Campbell, D. Wackeroth and J. Zhou, Phys. Rev. D **94**, no. 9, 093009 (2016).

[14] R. Frederix, S. Frixione, V. Hirschi, D. Pagani, H. S. Shao and M. Zaro, JHEP **1704**, 076 (2017).

[15] J. Currie, E. W. N. Glover and J. Pires, Phys. Rev. Lett. **118**, 072002 (2017).

[16] J. Currie, E. W. N. Glover, A. Gehrmann-De Ridder, T. Gehrmann, A. Huss and J. Pires, arXiv:1704.00923; J. Currie, E. W. N. Glover, A. Gehrmann-De Ridder, T. Gehrmann, A. Huss and J. Pires, arXiv:1705.08205.

[17] G. P. Salam, Eur. Phys. J. C **67**, 637 (2010).

[18] S. Chatrchyan *et al.* [CMS Collaboration], Phys. Rev. D **87**, 112002 (2013) Erratum: [Phys. Rev. D **87**, 119902 (2013)].

[19] G. Aad *et al.* [ATLAS Collaboration], JHEP **1405**, 059 (2014).

[20] V. M. Abazov *et al.* [D0 Collaboration], Phys. Lett. B **693**, 531 (2010).

[21] W. T. Giele, E. W. N. Glover and D. A. Kosower, Phys. Rev. D **52**, 1486 (1995).

[22] A. M. Sirunyan *et al.* [CMS Collaboration], arXiv:1705.02628 [hep-ex].

[23] M. Cacciari, G. P. Salam and G. Soyez, JHEP **0804**, 063 (2008).

[24] A. Gehrmann-De Ridder, T. Gehrmann and E.W.N. Glover, JHEP **0509**, 056 (2005); J. Currie, E.W.N. Glover and S. Wells, JHEP **1304**, 066 (2013).

[25] A. Daleo, T. Gehrmann and D. Maitre, JHEP **0704**, 016 (2007); A. Daleo, A. Gehrmann-De Ridder, T. Gehrmann and G. Luisoni, JHEP **1001**, 118 (2010); R. Boughezal, A. Gehrmann-De Ridder and M. Ritzmann, JHEP **1102**, 098 (2011); T. Gehrmann and P. F. Monni, JHEP **1112**, 049 (2011); A. Gehrmann-De Ridder, T. Gehrmann and M. Ritzmann, JHEP **1210**, 047 (2012).

[26] M. L. Mangano and S. J. Parke, Phys. Rept. **200**, 301 (1991).

[27] Z. Bern, L. J. Dixon and D. A. Kosower, Phys. Rev. Lett. **70**, 2677 (1993); Z. Bern, L. J. Dixon and D. A. Kosower, Nucl. Phys. B **437**, 259 (1995); Z. Kunszt, A. Signer and Z. Trocsanyi, Phys. Lett. B **336**, 529 (1994).

[28] E. W. N. Glover, C. Oleari and M. E. Tejeda-Yeomans, Nucl. Phys. B **605**, 467 (2001); E. W. N. Glover and M. Tejeda-Yeomans, JHEP **0105**, 010 (2001); Z. Bern, A. De Freitas and L. J. Dixon, JHEP **0203**, 018 (2002); C. Anastasiou, E. W. N. Glover, C. Oleari and M. E. Tejeda-Yeomans, Nucl. Phys. B **605**, 486 (2001); Phys. Lett. B **506**, 59 (2001); JHEP **0306**, 033 (2003); Z. Bern, A. De Freitas and L. J. Dixon, JHEP **0306**, 028 (2003). Erratum: [JHEP **1404**, 112 (2014)].

[29] C. Anastasiou, E. W. N. Glover, C. Oleari and M. E. Tejeda-Yeomans, Nucl. Phys. B **601**, 318 (2001); Nucl. Phys. B **601**, 341 (2001); Phys. Lett. B **506**, 59 (2001); A. De Freitas and Z. Bern, JHEP **0409**, 039 (2004).

[30] L. A. Harland-Lang, A. D. Martin, P. Motylinski and R. S. Thorne, Eur. Phys. J. C **75**, 204 (2015).